SKEW SHOCK WAVE ON THE INTERFACE BETWEEN TWO POLYTROPIC GASES

S. K. Andilevko

UDC 534.2

Break decay occurring in emergence of a skew shock wave on the surface separating polytropic gases at the side of the less dense of them is calculated. Both regular and irregular regimes of interaction are considered and the parameters of the gases for different reflection and refraction regimes are determined.

Break decay (BD) occurring in emergence of a skew shock wave ($D > c_1$, $D > c_5$) on the interface between two polytropic gases has already been studied earlier [1]. It was assumed that in the interaction of the skew shock wave (SSW) with the interface between a less and a more dense gas the BD on the contact surface (CS) is accompanied by formation of refracted and reflected shock waves (RrSW and RlSW, Fig. 1) up to the transition angle (or the angle of total refraction φ_t), when the regular reflection regime changes to an irregular one [1] in which instead of the RlSW a rarefaction wave (RW) starts to propagate over the less dense gas. This hypothesis allowed researchers to calculate BD for almost all contact angles between the SSW and CS. However, in numerical value, φ_t does not coincide with the other characteristic angle φ_c, at which behind the SSW the flow velocity becomes subsonic (Fig. 2a). It should be noted that for different D there are regions where $\varphi_t > \varphi_c$ and where $\varphi_t < \varphi_c$. In the second case one can indicate a shock-wave regime for angles $\varphi_t > \varphi > \varphi_c$, while in the first case we have to recognize irregular shockless reflection even before φ becomes equal to φ_t (since at $\varphi \geq \varphi_t$ solutions with an RlSW are impossible). Almost the same mechanism is used for calculation of BD in the interaction of an SSW with surfaces of solids and liquids, when the CS cannot be considered rigid; however, in this case there is no smooth transition to the limiting case of BD on a rigid wall, where in the sense of the problem calculated in [1], the angle of transition from regular to irregular reflection, accompanied by the appearance of a Mach wave (MW), could be used as φ_t. The present work is carried out in order to show that these inconsistencies are not fatal and can be eliminated within the hydrodynamic theory of shock waves.

Let ρ_1 and ρ_5 be the initial densities of two polytropic gases having a flat immovable CS ($p_1 = p_5$), on which an SSW emerges at the angle φ; here $\rho_1 < \rho_5$ (see Fig. 1). The polytrope indices of the gases are denoted by k and m, respectively. Regular interaction can be described by three systems of equations for media 2-4, following known procedures [1, 2]. Using the equations of state (of the polytrope) and the Rankine–Hugoniot relations, for each region of the gases separated by the break surfaces in a coordinate system connected with the point O ($q_1 = q_5 = D/\sin\varphi$), we can write down the corresponding systems of equations determining the flow parameters behind the front of the shock wave (SW): for medium 2 [2]:

$$p_2 = \frac{2\rho_1 q_1^2}{k+1}\sin^2\varphi - \frac{k-1}{k+1}p_1\,,\quad \frac{\rho_1}{\rho_2} = K(p_2/p_1) = \frac{k+1+(k-1)\,p_2/p_1}{k-1+(k+1)\,p_2/p_1}\,,$$

$$u_2 = q_1 \sin\varphi K(p_2/p_1)\,,\quad \theta_2 = \varphi - \arccos\sqrt{\left(\frac{1}{1+\tan^2\varphi K(p_2/p_1)^2}\right)}\,, \tag{1}$$

$$q_2 = \sqrt{q_1^2\cos^2\varphi + q_1^2\sin^2\varphi K(p_2/p_1)^2} = q_1\cos\varphi\sqrt{1+\tan^2\varphi K(p_2/p_1)^2}\,;$$

Scientific-Research Institute of Pulse Processes of the Belarusian State Scientific and Production Concern of Powder Metallurgy, Minsk, Belarus. Translated from Inzhenerno-Fizicheskii Zhurnal, Vol. 72, No. 2, pp. 210-217, March-April, 1999. Original article submitted April 3, 1998.

 1062-0125/99/7202-0186$22.00

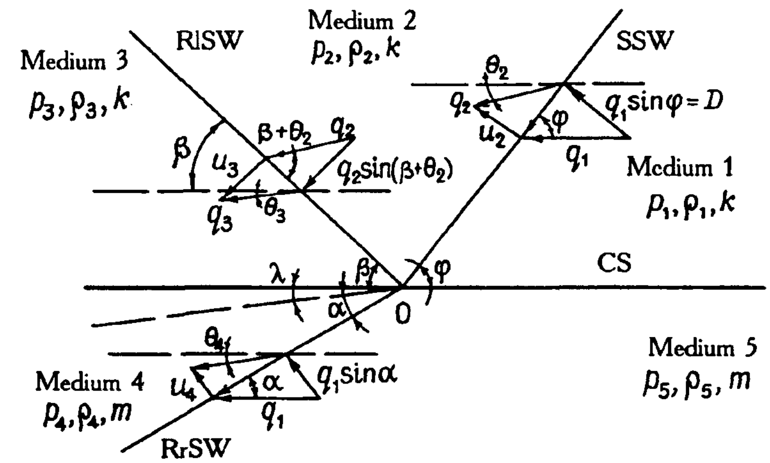

Fig. 1. Regular interaction of an SSW with the CS between light and heavy gases.

for medium 3:

$$p_3 = \frac{2\rho_2 q_2^2}{k+1}\sin^2(\beta+\theta_2) - \frac{k-1}{k+1}p_2\,, \quad u_3 = q_2\sin(\beta+\theta_2)\,K(p_3/p_2)\,,$$

$$\rho_3/\rho_2 = K(p_3/p_2)^{-1}\,, \quad \theta_3 = \arccos\sqrt{\left(\frac{1}{1+\tan^2(\beta+\theta_2)\,K(p_3/p_2)^2}\right)} - \beta\,, \tag{2}$$

$$q_3 = q_2\cos(\beta+\theta_2)\sqrt{1+\tan^2(\beta+\theta_2)\,K(p_3/p_2)^2}\,;$$

for medium 4:

$$p_4 = \frac{2\rho_5 q_1^2}{m+1}\sin^2\alpha - \frac{m-1}{m+1}p_1\,, \quad \theta_4 = \alpha - \arccos\sqrt{\left(\frac{1}{1+\tan^2\alpha M(p_4/p_1)^2}\right)}\,,$$

$$u_4 = q_1\sin\alpha M(p_4/p_1)\,, \quad \frac{\rho_5}{\rho_4} = M(p_4/p_1) = \frac{m+1+(m-1)p_4/p_1}{m-1+(m+1)\,p_4/p_1}\,, \tag{3}$$

$$q_4 = q_1\cos\alpha\sqrt{1+\tan^2\alpha M(p_4/p_1)^2}\,.$$

where M is a function. The total system of equations (1)-(3) consists of 15 equalities for determination of 17 unknown quantities: p_2, p_3, p_4, ρ_2, ρ_3, ρ_4, q_2, q_3, q_4, u_2, u_3, u_4, θ_2, θ_3, θ_4, β, and α. The two missing equations are obtained from the conditions of equality of the pressure and the normal components of the gas velocity on both sides of the CS:

$$p_4 = p_3\,, \quad q_3\sin\theta_3 = q_4\sin\theta_4\,. \tag{4}$$

The first of Eqs. (4) establishes a relation between the angles α and β:

$$\sin\alpha = \sqrt{\left(\frac{m+1}{k+1}\frac{\rho_2}{\rho_5}\left(\frac{q_2}{q_1}\right)^2\sin^2(\beta+\theta_2) - \frac{k-1}{k+1}\frac{m+1}{2}\frac{p_2}{\rho_5 q_1^2} + \frac{m-1}{2}\frac{p_1}{\rho_5 q_1^2}\right)}\,. \tag{5}$$

Since p_2, ρ_2, q_2, u_2, and θ_2 are determined in terms of initial parameters and the other 10 unknown quantities (except β and α) are determined only in terms of them and in terms of β and α, the second of Eqs. (4) is transformed into a transcendental equation for determination of the single unknown β:

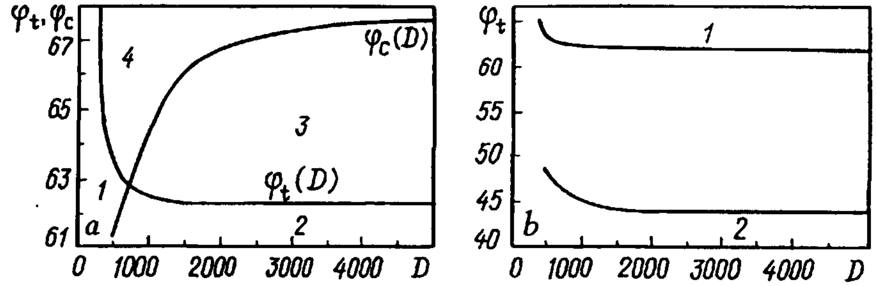

Fig. 2. Curves $\varphi_t(D)$ and $\varphi_c(D)$ obtained by the author (a) and $\varphi_c(D)$ obtained in [1] and calculated by the author (b): a) region of: 1) weak irregular reflection, 2) regular reflection, 3) strong irregular reflection, 4) strong shockless irregular reflection; b: 1) present data, 2) [1].

$$q_2 \cos(\beta + \theta_2) \sqrt{1 + \tan^2(\beta + \theta_2) K (p_3/p_2)^2} \times$$

$$\times \sin\left(\arccos\sqrt{\left(\frac{1}{1 + \tan^2(\beta + \theta_2) K (p_3/p_2)^2}\right)} - \beta\right) =$$

$$= q_1 \cos\alpha \sqrt{1 + \tan^2\alpha\, M (p_4/p_1)^2} \sin\left(\alpha - \arccos\sqrt{\left(\frac{1}{1 + \tan^2\alpha\, M (p_4/p_1)^2}\right)}\right). \tag{6}$$

Having solved (6) numerically with respect to β, we determine parameters (1)-(3). The slope of the CS is

$$\lambda = \arctan\frac{q_4 \sin\theta_4}{q_1}. \tag{7}$$

The procedure described above leads to real solutions only if after the SSW the gas flow is supersonic, i.e., when

$$\frac{q_2}{c_2} \geq 1 \quad \text{or} \quad \operatorname{ctan}\varphi \geq \sqrt{\left(\frac{2kK(p_2/p_1)}{k+1} - \frac{k-1}{k+1}\frac{kp_1}{\rho_1 D^2} K(p_2/p_1) - K(p_2/p_1)^2\right)}. \tag{8}$$

For strong SW ($p_2 >> p_1$, $D >> c_1$) $K(p_2/p_1) = (k-1)/(k+1)$ and (8) is transformed into

$$\varphi \leq \varphi_c = \arctan\sqrt{\left(\frac{k-1}{k+1}\right)}. \tag{9}$$

The curve $\varphi_c(D)$ is shown in Fig. 2a for $\rho_1 = 1.29$ kg/m^3, $\rho_5 = 3.747$ kg/m^3, $k = 1.4$, and $m = 5/3$ (the air–krypton pair [1]). An analysis of the solution of (1)-(3) shows that there is an angle φ_t for which the reflection wave disappears. The authors of [1] call it the angle of change of the reflection regime, assuming that after it the RISW should be replaced by an RW. However, Fig. 2a shows that there is a difference between the angles φ_t and φ_c, which increases with D. In the region between these two angles there is no simultaneous solution of systems (1)-(3); however, in general, a shock-wave solution does exist. It can be found assuming that as in the case with a rigid wall rotation of the velocity vector of the gas flow q_1 that is not compensated by the RISW results in separation of the contact point (CP) from the CS and the appearance of a three-wave configuration typical of Mach reflection. In the general case, the Mach wave is not flat. However, like any curve, it can be continuously divided into a series of straight sections, which approximate this curve more accurately, the larger their number. Each of these "pieces" of the Mach wave can be considered as a plane SW. Since according to experimental data of [3, 4], the Mach wave is a slightly sloping smooth curve, the series of sections approximating it can be characterized by the angles made by its extreme sections with a horizontal line at the triple point O' and at the point O (Fig. 3a), i.e., by the angles

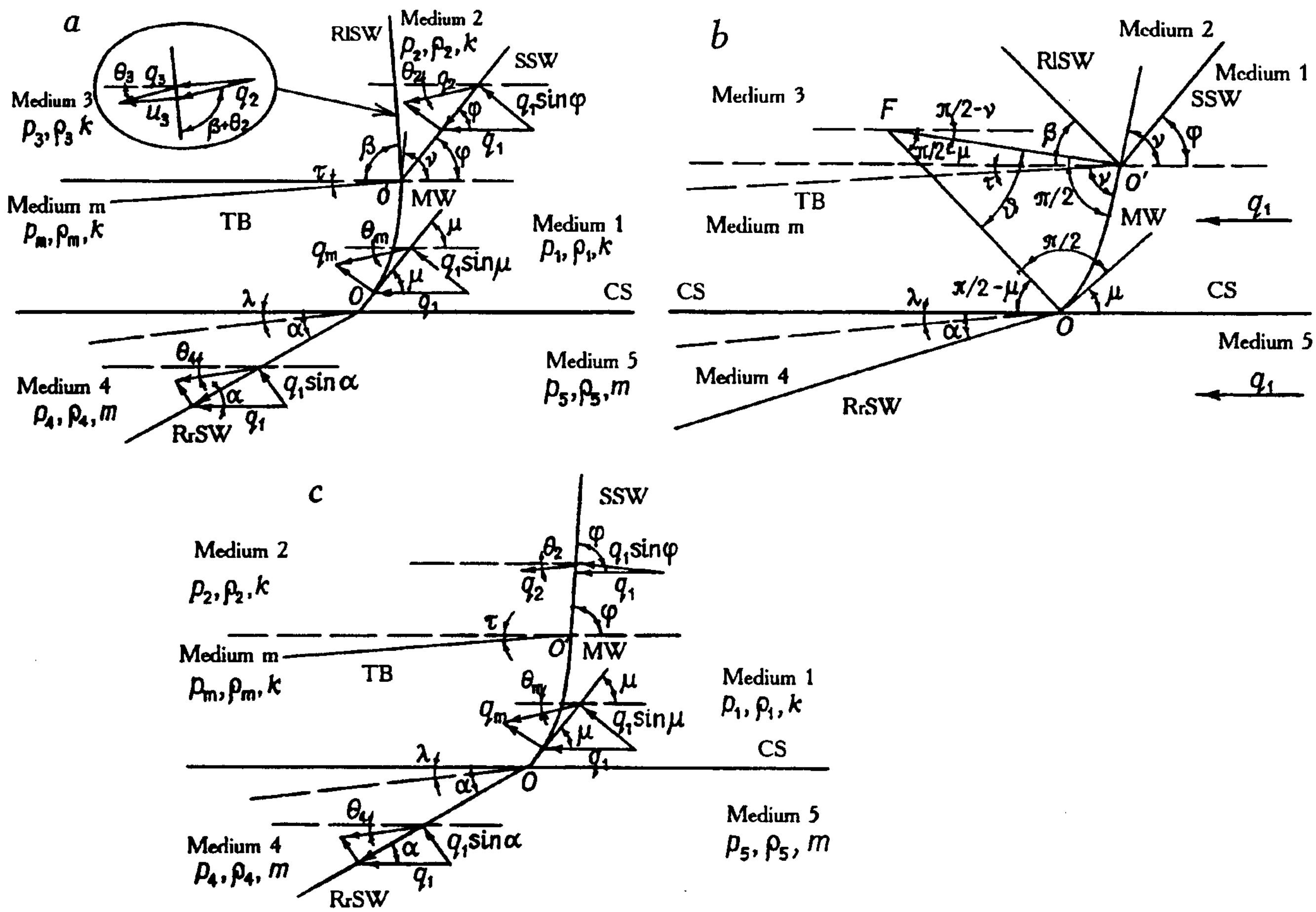

Fig. 3. Scheme of break decay in the case of strong irregular interaction for determination of the parameters of: a) the gas behind the shock-wave front in the case of an SIR; b) the approximating sector in the case of an SIR and SSIR; c) the gas behind the SW front in the case of SSIR.

at which the Mach wave enters the points O' and O. Thus, if we find these angles, we can determine the orientation of the Mach wave, its change with changing φ and D, and, consequently, the parameters of the gas flow behind it. The solution for the configuration near the triple point O' (Fig. 3a) is known [3, 5] and is obtained by simultaneous solution of the systems of equations (1), (2), and

$$p_\nu = \frac{2\rho_1 q_1^2}{k+1}\sin^2\nu - \frac{k-1}{k+1}p_1\,, \quad u_\nu = q_1 \sin\nu K(p_\nu/p_1)\,,$$

$$\rho_\nu/\rho_1 = K(p_\nu/p_1)^{-1}\,, \quad \theta_\nu = \nu - \arccos\sqrt{\left(\frac{1}{1+\tan^2\nu\, K(p_\nu/p_1)^2}\right)}\,, \tag{10}$$

$$q_\nu = q_1\cos\nu\sqrt{1+\tan^2\nu\, K(p_\nu/p_1)^2}\,.$$

The total system (1), (2), and (10) includes 15 equations for determination of 17 unknown quantities: p_2, p_3, p_ν, ρ_2, ρ_3, ρ_ν, q_2, q_3, q_ν, u_2, u_3, u_ν, θ_2, θ_3, θ_ν, β and ν. This system is closed by the conditions of equality of the pressure and the normal components of the flow velocity vectors on both sides of the tangential break (TB) (Fig. 3a)

$$p_\nu = p_3\,, \quad q_3\sin\theta_3 = q_\nu\sin\theta_\nu\,. \tag{11}$$

Just as in the previous case a relation between β and ν is found from the first equality of (11), and the second is transformed into a transcendental equation for calculation of β:

$$\sin \nu = \sqrt{\left(\frac{\rho_2}{\rho_1}\left(\frac{q_2}{q_1}\right)^2 \sin^2(\beta + \theta_2) - \frac{k-1}{2}\frac{p_2 - p_1}{\rho_1 q_1^2}\right)},$$

$$q_2 \cos(\beta + \theta_2)\sqrt{1 + \tan^2(\beta + \theta_2) K(p_3/p_2)^2} \times$$

$$\times \sin\left(\arccos\sqrt{\left(\frac{1}{1 + \tan^2(\beta + \theta_2) K(p_3/p_2)^2}\right)} - \beta\right) =$$

$$= q_1 \cos \nu \sqrt{1 + \tan^2 \nu K(p_\nu/p_1)^2} \sin\left(\nu - \arccos\sqrt{\left(\frac{1}{1 + \tan^2 \nu K(p_\nu/p_1)^2}\right)}\right). \quad (12)$$

For calculation of the two-wave structure near the point O (Fig. 3a), the system of equations (3) is solved simultaneously with a system similar to (10) for the angle μ (Fig. 3a):

$$p_m = \frac{2\rho_1 q_1^2}{k+1}\sin^2\mu - \frac{k-1}{k+1}p_1, \quad u_m = q_1 \sin\mu K(p_m/p_1),$$

$$\rho_m/\rho_1 = K(p_m/p_1)^{-1}, \quad \theta_m = \mu - \arccos\sqrt{\left(\frac{1}{1 + \tan^2\mu K(p_m/p_1)^2}\right)}, \quad (13)$$

$$q_m = q_1 \cos\mu\sqrt{1 + \tan^2\mu K(p_m/p_1)^2};$$

with equality of the pressure and the normal projection of the velocity on both sides of the CS:

$$p_m = p_4, \quad q_4 \sin\theta_4 = q_m \sin\theta_m. \quad (14)$$

This can be used to find a relation between α and μ:

$$\sin\alpha = \sqrt{\left(\frac{m+1}{k+1}\frac{\rho_1}{\rho_5}\sin^2\mu - \frac{k-1}{k+1}\frac{m+1}{2}\frac{p_1}{\rho_5 q_1^2} + \frac{m-1}{2}\frac{p_1}{\rho_5 q_1^2}\right)} \quad (15)$$

and to obtain a transcendental equation for determination of μ:

$$\cos\mu\sqrt{1 + \tan^2\mu K(p_m/p_1)^2}\sin\left(\mu - \arccos\sqrt{\left(\frac{1}{1 + \tan^2\mu K(p_3/p_2)^2}\right)}\right) =$$

$$= \cos\alpha\sqrt{1 + \tan^2\alpha M(p_4/p_1)^2}\sin\left(\alpha - \arccos\sqrt{\left(\frac{1}{1 + \tan^2\alpha M(p_4/p_1)^2}\right)}\right). \quad (16)$$

The angle of rotation of the CS is determined from (7), and the slope of the TB to the horizontal line, from

$$\tau = \arctan\frac{q_\nu \sin\theta_\nu}{q_1}. \quad (17)$$

The combined system (3) and (13) can also be used to calculate φ_t, provided that $\varphi = \mu = \varphi_t$. Then, instead of (15), we obtain a relation relating α and φ_t:

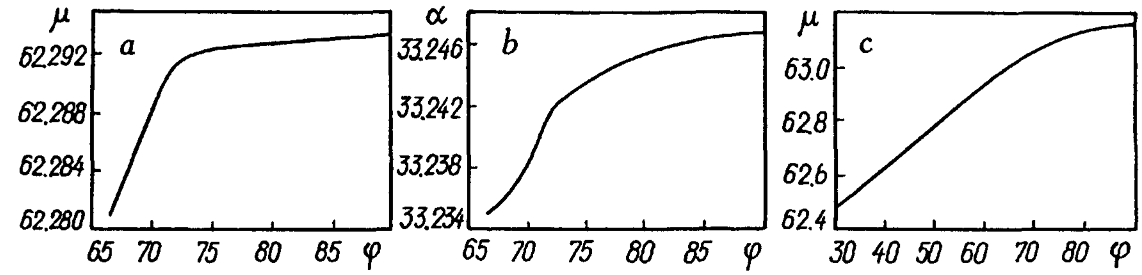

Fig. 4. Curves in the range $\varphi_t \leq \varphi_c \leq \varphi$: a) $\mu(\varphi)$ at $D = 2000$ m/sec; b) $\alpha(\varphi)$ at $D = 2000$ m/sec; c) $\mu(\varphi)$ at $D = 500$ m/sec.

$$\sin\alpha = \sin\varphi_1 \sqrt{\left(\frac{m+1}{k+1}\frac{\rho_1}{\rho_5}\left(\frac{m-1}{2} - \frac{k-1}{k+1}\frac{m+1}{2}\right)\frac{p_1}{\rho_5 D^2}\right)}, \tag{18}$$

and the value of φ_t is found directly from (16), where μ should be replaced by φ_t, whose dependence on D is shown in Fig. 2a. The general form and the ratio of the curves $\varphi_t(D)$ and $\varphi_c(D)$ are valid for almost all corresponding pairs of gases. It should be noted that the results of calculation of φ_t from the present data and those calculated from the formula presented in [1] differ from each other in numerical value, although they coincide in the general form of the curve (Fig. 2b). For the air–krypton pair, at angles $\varphi > \varphi_t$ determined from [1], regular reflection is still possible: for $D = 2000$ m/sec, according to [1], $\varphi_t \approx 44.1°$, but regular reflection is possible even at $\varphi = 50°$; in this case $\beta \approx 87.9°$, $\alpha \approx 47.9°$, and $q_2/c_2 \approx 1.5$. The present calculations give $\varphi_t \approx 62.3°$, and for all angles exceeding this value only irregular reflection is observed. For example, for the same gases at $D = 2000$ m/sec and $\varphi = 63.16°$ ($\varphi_c \approx 66.8°$, and $\varphi_t \approx 62.38°$), $\nu \approx 80.162°$, $\mu \approx 62.281°$, $\beta \approx 72.938°$, and $\alpha \approx 33.233°$, and irregular reflection is observed with an RlSW determined by the angle β and an MW bounded by the angles μ and ν. The angle α belongs to the RrSW, and for all waves the Mach numbers exceed 1. For the present case there is no solution for regular reflection.

Analyzing the present results for irregular reflection written in terms of the simultaneous solution of systems (1), (2), (10) and (3), (13) in the range $\varphi_t < \varphi < \varphi_c$, it should be noted that for a strong irregular regime (SIR), at the triple point O' the slope of the MW ν always exceeds μ (but not $\pi/2$), and hence it follows that the convex side of the curved MW (at $\mu \neq \nu$ it is impossible to connect the points O and O' shown in Fig. 3a by a straight line) faces the incident flow. If the MW is approximated by an arc of a circle (which is possible since the MW is mildly sloping and smooth [4, 6], Fig. 3b), the sector (FOO') bounded by it is determined by the angle $\vartheta = \pi/2 - \mu - (\pi/2 - \nu) = \nu - \mu$. The center of the approximating circle F is located to the left of O and O', and since $\nu \leq \pi/2$ it is always above the TB. The parameters of the flow change smoothly along the curve OO' and this change is determined by the local angle of intersection of the MW by the streamline.

When $\varphi \geq \varphi_c > \varphi_t$, the flow behind the SSW becomes subsonic, and strong shockless irregular reflection (SSIR) is observed. The reflected wave is absent (behind the SSW the flow is subsonic, Fig. 3c), and the angle at which the MW enters the point O can be obtained by simultaneous solution of system (3) and (13) under conditions (14)-(16). Plots of μ and α versus φ are shown in Fig. 4a, b for the air–krypton pair at $D = 2000$ m/sec and $\varphi \geq \varphi_c > \varphi_t$. In SSIR the angle μ is always smaller than φ (see Fig. 3c) and $\vartheta = \pi/2 - \mu - (\pi/2 - \varphi) = \varphi - \mu$. The surface of the tangential break has the slope

$$\tau = \arctan\frac{q_2 \sin\theta_2}{q_1}. \tag{19}$$

For small D ($\varphi_t > \varphi_c$, Fig. 2a) regular reflection exists only for $\varphi < \varphi_c$ or, as in the case of $D = 500$ m/sec, does not exist at all. The curve $\mu(\varphi)$ is shown in Fig. 4c for $D = 500$ m/sec. At $\varphi < \varphi_t$, the angle μ is always larger than φ, and a weak regime of irregular reflection (WRIR) is realized ($\varphi_c < \varphi < \varphi_t$, Fig. 5a). The angle of the sector with the approximating curve OO' is $\vartheta = \pi/2 - \varphi - (\pi/2 - \mu) = \mu - \varphi$; its center F is always located to the right

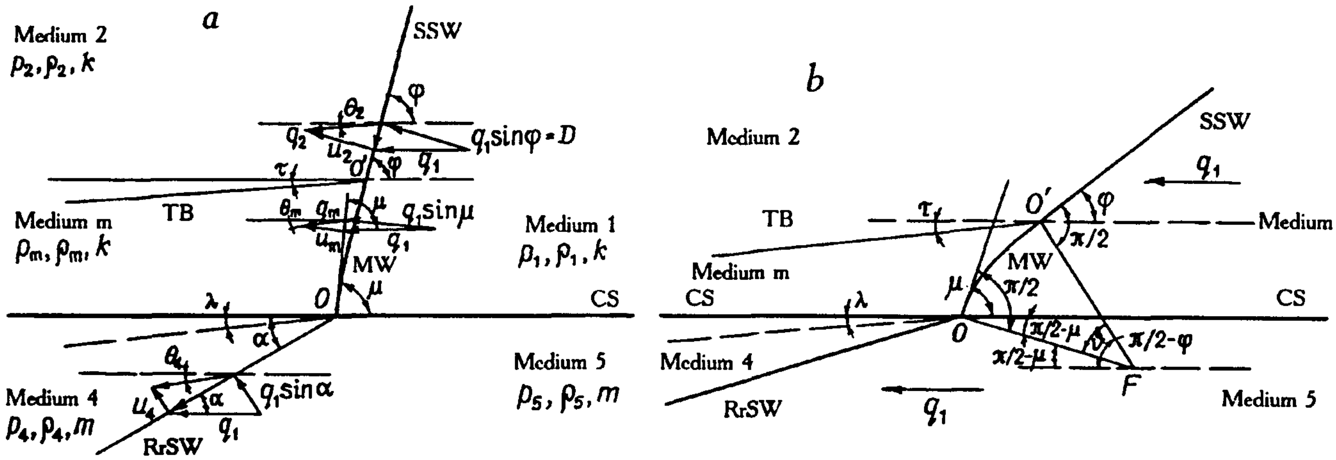

Fig. 5. Schemes of break decay in the case of weak irregular interaction for determination of the parameters of: a) the gas behind the SW front and b) the approximating sector for the curve.

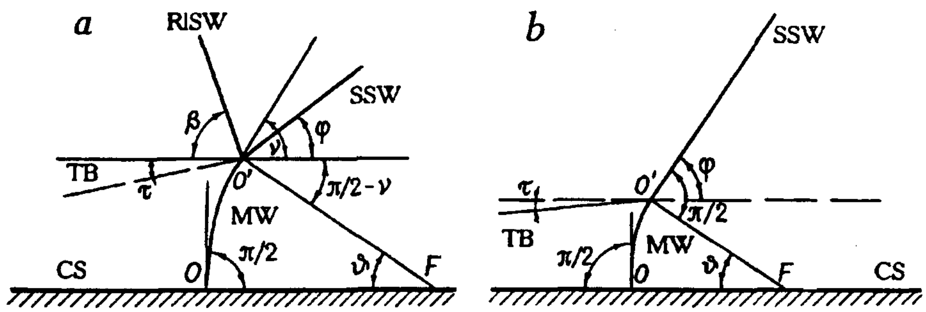

Fig. 6. Schemes of construction of irregular reflection from a rigid surface: a) strong reflection; b) weak reflection.

of O under the CS (Fig. 5b). The turn of the TB is determined from (19). At $\varphi > \varphi_t$ SSIR is observed ($\mu < \varphi$), and when these angles are equal (see Fig. 4c), total refraction is realized, when $\mu \equiv \varphi \equiv \varphi_t$.

This phenomenon should be observed not only on a gas–gas interface but also on any interface of this type (gas–solid, gas–liquid, liquid–liquid, and even solid–solid interfaces); however, this problem needs further investigation. Here, it should be noted that the fact that the impedance of the "lower" medium exceeds that of the "upper" is of fundamental importance. Here, the concept of rigidity acquires physical meaning, since at $q_1/c_5 \geq 1$, the CS cannot be considered rigid, and on it the BD should be calculated following the above procedure. If $q_1/c_5 < 1$ (but $D > c_1$), the CS can be assumed rigid, and in the region of regular reflections the flow is determined by simultaneous solution of the systems of equations (1) and (2) with the additional condition $\theta_3 = 0$ (the flow should be parallel to the rigid surface behind the CP), which involves a new parameter, the critical angle of regular reflection θ_c [3, 5], typical only of a rigid surface. The angle φ_t is not yet determined for it, since to do this, it is necessary to ascertain its dependence on the rigidity, and as before, the angle φ_c is determined from (8). However, the system of construction of irregular reflection allows us to make certain conclusions relative to the angle φ_t even now: since for a rigid wall $\mu = \pi/2$ for both strong and weak irregular reflection, which is caused by requirements of parallelism of the gas flow at the wall, SSIR cannot be realized, since in this case φ should exceed μ. Thus, when φ exceeds θ_c, the reflection regime changes and for $\theta_c < \varphi < \varphi_c$ an SIR is observed, for which it is sufficient to determine the angle ν at which the MW enters the triple point O' and the parameters of the gas behind the SSW and the RlSW (Fig. 6a), which can be done by simultaneous solution of systems (1), (2), and (10) with conditions (11) and (12). In this case ν is always smaller than $\pi/2$. The approximating sector of the circle has the angle $\vartheta = \pi/2 - \nu$, and the point F of the center of curvature lies on the CS to the right of the point O'. The slope of the curve changes smoothly, which determines the corresponding smooth change in the parameters of the gas behind the front of the MW, and the convex side of the curve is turned to the left of O. At $\varphi \geq \varphi_c$ the RlSW disappears (Fig. 6b) and the SIR is replaced by a WRIR. This regime is preserved for all $\pi/2 \geq \varphi \geq \varphi_c$ (i.e., a single possible value $\varphi_t \equiv \pi/2$ remains for the angle φ_t). It should be noted that for almost all polytropic gases the critical angle of change in the reflection regime θ_c is smaller than φ_c for relatively large D. For small D only a WRIR always exists. Since $\mu = \pi/2$, for a WRIR a graphical solution consists in constructing the approximating sector with the angle $\vartheta = \pi/2 - \varphi$, the slope of the tangent to whose surface varies smoothly from $\pi/2$ to φ, determining thereby the smooth variation of the flow parameters behind the MW up to its entry into the point O'. For a WRIR the point F is located on the CS to the right of the point O (Fig. 6b). Behind the front of the MW, the parameters of the gas are determined by the angle contact with the MW and the initial parameters of the problem for each streamline. All this allows us to combine a wide range of problems of calculation of the interaction of an SSW with a CS with various rigidity into one problem and to obtain their solution for many materials. In particular, the author is planning to consider the interaction of an SSW with various contact surfaces.

Thus, the present study gives a consistent picture of irregular interaction of a shock wave with the CS of two polytropic gases for the case where an SSW moves from a lighter gas to a heavier one. The dependence of the type of reflection on the mutual combination of two angles (the angle of total reflection and the angle of change in the supersonic flow behind the SSW to a subsonic flow) is ascertained. It is also found that the angle of total reflection determines the orientation of the curvature of the MW and its change with change in the contact angle. As one would expect, the second angle determines the change in the shock reflection (when the RISW exists) to a shockness one (when the RISW is absent).

In conclusion, the author wants to express his gratitude to G. S. Romanov, V. A. Shilkin, and V. V. Selyavko for their useful and active participation in discussion of this work.

NOTATION

D, shock-wave velocity; c, velocity of sound in the medium; p, pressure; q, total velocity of the gas flow in a coordinate system connected with the point of intersection of the skew shock wave with the surface; u, component of the gas-flow velocity normal to the shock-wave front; k, polytrope index of the lighter gas; m, polytrope index of the heavier gas; ρ, density; α, slope of the refracted shock wave to the CS; β, slope of the reflected shock wave to the CS; φ, slope of the skew shock wave to the CS; λ, angle of rotation of the surface; τ, angle of rotation of the tangential break; μ, angle at which the Mach wave enters the contact point of the skew shock wave with the CS; ν, angle of the Mach wave at the triple point; θ, angle of rotation of the vector of the total gas velocity behind the shock-wave front; ϑ, angle of the sector approximating the surface of the Mach wave; θ_c, critical angle of change in the reflection regime for a rigid surface. Subscripts: 1, initial parameters of the light gas (medium 1); 2, parameters of medium 2 (immediately behind the skew shock wave); 3, parameters of medium 3 (immediately behind the reflected shock wave); 4, parameters of medium 4 (immediately behind the refracted shock wave); 5, initial parameters of the heavier gas (medium 5); c, critical angle at which the supersonic flow behind the skew shock wave changs to a subsonic flow; t, angle of total refraction or transition angle between regular and irregular interaction regimes; m, parameters of the gas in the lower part of the Mach wave at the angle μ; v, parameters of the gas in the upper part of the Mach wave at the angle ν.

REFERENCES

1. C. Polaček and R. I. Sieger, in: Fundamentals of Gas Dynamics (ed. by G. Emmons) [Russian translation], Moscow (1963), pp. 446-489.
2. F. A. Baum, L. P. Orlenko, K. P. Stanyukovich, V. P. Chelyshev, and V. B. Shekhter, Physics of Explosion [in Russian], Moscow (1975).
3. W. Bleackney and A. Taub, Rev. Mod. Phys., 21, No. 4, 584-605 (1949).
4. L. V. Al'tshuler, S. B. Kormer, A. A. Bakanova, et al., Zh. Éksp. Teor. Fiz. 41, No. 511, 1382-1393 (1961).
5. K. P. Stanyukovich, Unsteady Motions of Continua [in Russian], Moscow (1955).
6. G. M. Arutyunyan and L. V. Karchevskii, Reflected Shock Waves [in Russian], Moscow (1973).